Article

Chinese Science Bulletin

Electronics

February 2012 Vol.57 No.4: 409–412
doi: 10.1007/s11434-011-4821-4

Character and fabrication of $Al/Al_2O_3/Al$ tunnel junctions for qubit application

SHEN DanDan, ZHU Ran, XU WeiWei*, CHANG JunJie, JI ZhengMing, SUN GuoZhu, CAO ChunHai & CHEN Jian

Research Institute of Superconductor Electronics, Nanjing University, Nanjing 210093, China

Received March 18, 2011; accepted September 20, 2011

The superconductive Josephson junction is the key device for superconducting quantum computation. We have fabricated $Al/Al_2O_3/Al$ tunnel junctions using a double angle evaporation method based on a suspended shadow mask. The Al_2O_3 junction barrier has been formed by introducing pure oxygen into the chamber during the fabrication process. We have adjusted exposure conditions by changing either the oxygen pressure or the oxidizing time during the formation of tunnel barriers to control the critical current density J_c and the junction specific resistance R_c. Measurements of the leakage in $Al/Al_2O_3/Al$ tunnel junctions show that the devices are suitable for qubit applications.

$Al/Al_2O_3/Al$ junctions, electron beam evaporation, superconducting qubit

Citation: Shen D D, Zhu R, Xu W W, et al. Character and fabrication of $Al/Al_2O_3/Al$ tunnel junctions for qubit application. Chin Sci Bull, 2012, 57: 409–412, doi: 10.1007/s11434-011-4821-4

In recent years, superconducting devices, such as superconducting Josephson junctions [1], filters [2–5], single photon detector [6] and hot electron bolometer (HEB) mixer [7] have attracted a great deal of interest in China. Important aspects to qubit applications are Josephson junctions and Superconducting Quantum Interference Device (SQUID) [8–12]. Quantum computation entails a new computation system that exceeds its classical counterpart. It is anticipated there will be an exponential speed up in solving problems which are difficult for classical computers, such as prime factorization. This prospect has fuelled much research into various experimental realizations of a quantum computer. Superconducting quantum computation is a viable and scalable approach to achieving a quantum computation scheme. Because of their solid state nature, their macroscopic phase coherence and their similarity to conventional semiconductor circuits, Josephson junction circuits are a promising technology within superconducting quantum computation schemes [13–16]. A typical flux qubit [16–19] consists of an isolated superconductive junction and a SQUID. In a SQUID the tunnel junctions are arranged in parallel to form a superconducting loop. The superconductive Josephson junction is the key device for superconducting quantum computation. The most commonly used materials for Josephson junction qubits are Aluminum (Al) and Niobium (Nb), because of the purity of their superconducting state as well as their relatively low transition temperatures (T_c = 1.2 K and 9.3 K, respectively) [20]. We have chosen to work with aluminum for several reasons. Firstly, high quality aluminum oxide has been shown to be less detrimental to Josephson junction qubits than other materials [21], with longer coherence times seen in aluminum-based devices [22]. Also, the fabrication of Al is flexible because of the fact that its melting point (660°C) is significantly lower than that of other popular superconducting materials, such as Nb (2477°C).

For qubit applications, we have explored the electronic properties of the $Al/Al_2O_3/Al$ tunnel junction, including the critical current density J_c and the junction specific resistance R_c, which depend on the oxygen pressure and the oxidation

*Corresponding author (email: wwxu@nju.edu.cn)

© The Author(s) 2012. This article is published with open access at Springerlink.com

time during the formation of the tunneling barrier. We have used the double angle evaporation technique [23] to fabricate the $Al/Al_2O_3/Al$ tunnel junctions. This technique has the advantage of allowing for the creation of small junction overlaps with sizes down to the submicron level. Likewise, this technique relies on a relatively simple process that does not involve breaking the vacuum. To create the small junction overlaps, we have evaporated aluminum at an angle with respect to the substrate. Factors that may limit the coherence time in flux qubit systems are the dissipation and the Johnson noise, because of sub-gap leakage in the junction. In this work, we report measurements of the sub-gap leakage in $Al/Al_2O_3/Al$ tunnel junctions and DC-SQUIDs. We have found that the devices have a low level of dissipation (less than 1%), which is suitable for qubit applications.

1 Fabrication of the $Al/Al_2O_3/Al$ tunnel junctions with controllable junction overlaps

Firstly, we fabricated a suspended shadow mask using a bilayer of photolithographic resist. We used a bottom layer of pre-sensitized resist (LOR10B) and a top layer of high resolution EBL resist (495PMMAC8). Then, we deposited two layers of aluminum (purity = 99.999%) using e-gun evaporation at different angles with respect to the substrate. Finally, we introduced high purity oxygen (purity = 99.99%) to the chamber where a sample stage was situated to form the tunneling barrier between the evaporation steps. The sample stage was attached to a rotational motor, allowing for titling of the sample from 0 to 90 degrees. For better orientation, the vacuum pressure was kept lower than 10^{-5} Pa. The substrate was placed roughly 80 cm from the evaporation source to ensure the aluminum was evaporated straight to the substrate. The area of junction overlaps can be calculated from the height of the bottom layer and the evaporation angles. In our experiments, junction overlaps ranging from 1 to 8 μm^2 were successfully fabricated (as shown in Figure 1).

It is critical to attain uniform and electrically continuous films for high quality barriers. Atomic force microscopy (AFM) was used for nanoscale imaging of the Al films. We have measured the Root Mean Square (RMS) value of the surface roughness for different thickness Al films deposited at different rates (as shown in Tables 1 and 2). The results show that the thinner Al films have smoother surfaces, whereas the depositing rate does not significantly affect the surface roughness. Each of the layers of aluminum film in our fabrication process were 100 nm thick and deposited at a rate of 0.2 nm/s with a critical current density of $J_c \approx 1\times10^5$ A/cm^2.

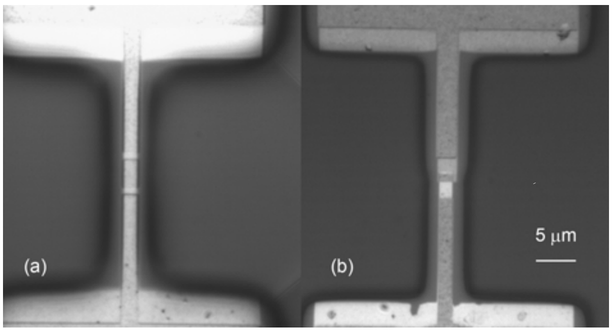

Figure 1 SEM photo of junctions with junction overlaps of roughly 8 μm^2 (sample a) and 1 μm^2 (sample b).

2 Controllable electronic-properties of $Al/Al_2O_3/Al$ tunnel junctions

Important requirements for achieving superconducting qubits include attaining suitable electronic properties, such as the critical current density J_c, the energy gap V_g and the subgap current I_c, which depend on the junction barrier quality. Oxygen-doped aluminum has long been used to significantly alter the superconducting energy gap from the bulk value. To discover the best conditions for junction barrier formation, we have adjusted the exposure conditions by changing either the oxygen pressure or the oxidizing time to obtain different barrier thicknesses. Since the tunnel junction resistance R_J is inversely proportional to the area of the junction, then the junction specific resistance R_c (the product of the tunnel junction resistance R_N and the junction area) is used as a characteristic figure [24].

Samples oxidized under oxygen pressures of $P = 25$ Pa for different oxidizing times have been fabricated to examine the relationship between the electronic properties of $Al/Al_2O_3/Al$ tunnel junctions and the oxidizing time t. We have found that the electronic properties are essentially independent of the oxidation time t when it is longer than 5 min, as shown in Table 3. As a consequence, attempts to find the functionality of the barrier thickness with respect to the oxidizing time will fail in certain conditions.

In Figures 2 and 3, we have plotted J_c and R_c versus the oxygen pressure for nine samples. The nine samples were

Table 1 RMS of surface roughness of aluminum films deposited at the same rate (0.1 nm/s) for various thicknesses

Thickness (nm)	RMS (nm)
50	2.469
100	4.33
200	8.71

Table 2 RMS of surface roughness of 100 nm thick aluminum films deposited at different rates

Depositing rate (nm/s)	RMS (nm)
0.7	4.483
0.35	4.487
0.08	4.33

Table 3 J_c and R_c of $Al/Al_2O_3/Al$ tunnel junctions oxidized with different oxidizing times *t* are essentially constant. The samples were oxidized under an oxygen pressure *P*=25 Pa at room temperature

Sample	Oxidation time (min)	J_c (A/cm^2)	R_c ($\Omega\ \mu m^2$)
1	5	30	800
2	5	40	1000
3	10	25	820
4	10	30	800
5	20	25	1000
6	20	30	800
7	20	14	1500

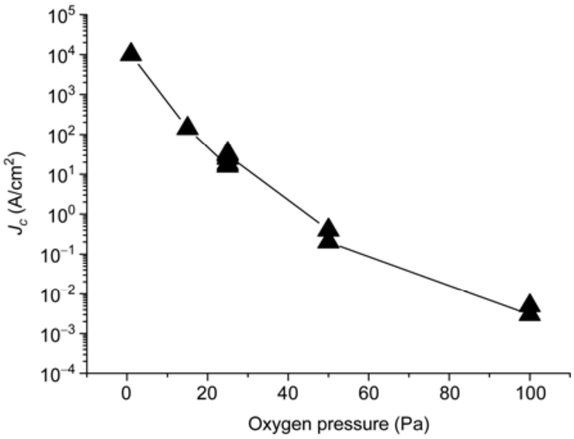

Figure 2 J_c and R_c of nine $Al/Al_2O_3/Al$ tunnel junctions plotted as a function of oxygen pressure *P*. The nine samples were oxidized for $t = 20$ min under different oxygen pressures *P* at room temperature.

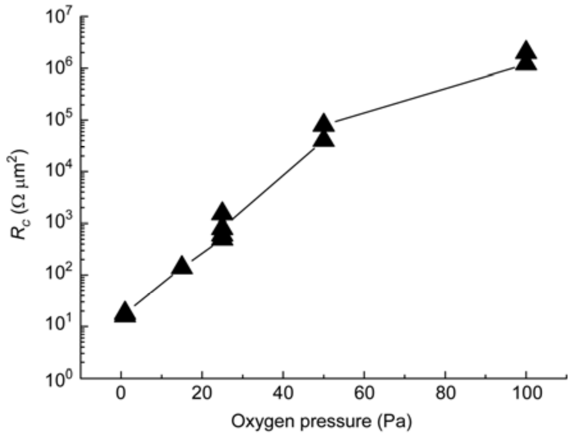

Figure 3 J_c and R_c of nine $Al/Al_2O_3/Al$ tunnel junctions plotted as a function of oxygen pressure *P*. The nine samples were oxidized for $t = 20$ min under different oxygen pressures *P* at room temperature.

fabricated for $t = 20$ min under different oxygen pressures at room temperature. On a logarithmic scale, the critical current density J_c is nearly linear with respect to the oxygen pressure between 1–50 Pa. We see a similar relationship for the junction specific resistance R_c. For oxygen pressures greater than 50 Pa, the barrier thickness increases more slowly. This feature may be caused by coverage of the oxidized Al preventing further oxygen contact with the Al. To study the relationship between the electronic properties and the exposure conditions for qubit applications, we chose to fabricate the $Al/Al_2O_3/Al$ tunnel junctions under 25 Pa for 5 min. Ultimately, $Al/Al_2O_3/Al$ tunnel junctions with controllable electronic properties can be easily prepared using different degrees of oxygen exposure between 1–50 Pa. Under these conditions, the system is capable of current controlling for qubit applications.

3 Characters of $Al/Al_2O_3/Al$ tunnel junctions and DC-SQUIDs

The $Al/Al_2O_3/Al$ tunnel junctions were measured in liquid helium (at 0.3 K) using a refrigeration system produced by OXFORD INSTRUMENTS (PT403-2440301). We have implemented a DC four-probe resistance measurement technique to discover the *I-V* characteristics up to a few μV and nA of bias.

In Figure 4, we show an image of the *I-V* curve of an $Al/Al_2O_3/Al$ junction measured at 0.3 K. The junction area is about 1 μm^2. The *I-V* curve displays a suppressed critical current because of environmental noise. The actual critical current, estimated from the switching current, is $I_c \approx 0.5$ μA. The energy gap is $V_g \approx 0.39$ mV and the junction specific resistance is $R_c \approx 500\ \Omega$. The sub-gap current is about 2.5 nA at 300 mK, approximately 0.5% of the superconducting current.

We have also made a DC-SQUID consisting of two $Al/Al_2O_3/Al$ Josephson junctions in parallel enclosed in a small superconducting loop (as shown in Figure 5). The area of the loop is $40\times40\ \mu m^2$ with a film width and thickness of 4 μm and 200 nm, respectively. The *I-V* curve of the DC-SQUID measured at a temperature of 20 mK has shown that the critical current of the DC-SQUID is $I_c \approx 2.1$ μA and the sub-gap current is about 0.007 μA, approximately 0.33% of the superconducting current.

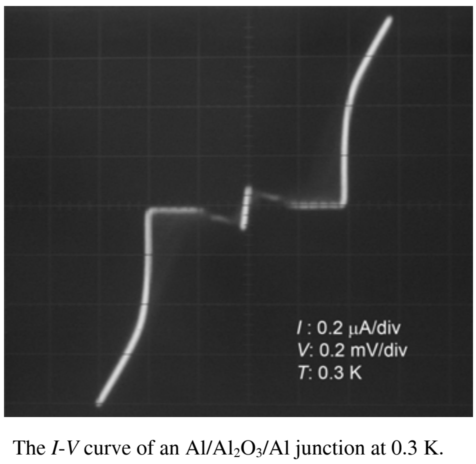

Figure 4 The *I-V* curve of an $Al/Al_2O_3/Al$ junction at 0.3 K.

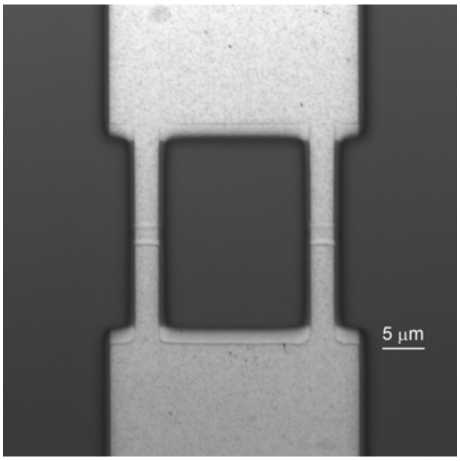

Figure 5 SEM photo of a DC-SQUID.

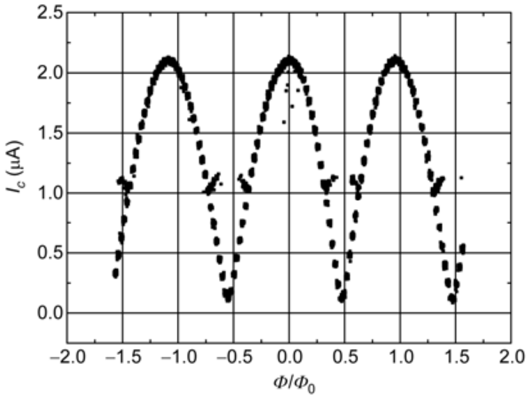

Figure 6 The current I_c, modulated by the external flux, measured at 20 mK.

An external flux F applied to the superconducting loop induced a persistent current (as shown in Figure 6):

$$I_s = I_c \sin\left(2\pi\Phi/\Phi_0\right). \quad (1)$$

The DC-SQUID is a sensitive detector that can, in certain arrangements, measure the value of the flux with a resolution of a few $\mu\Phi$ and can be applied to detect flux change in the flux qubit. As shown in Figure 6, we have measured the external magnetic field to be $B \approx 2.0\times10^{-4}$ T.

4 Conclusion

High quality $Al/Al_2O_3/Al$ tunnel junctions were successfully fabricated by controlling the barrier layer preparation conditions of specific parameters. The fabricated tunnel junctions that have a low level of dissipation (less than 1%) are suitable for qubit applications. This work has provided a good foundation for the preparation of circuits of superconducting quantum bits.

1 Xu W W, Chen J, Kang L, et al. Extraction of the spectral information of terahertz signals using superconducting Josephson junction. Chin Sci Bull, 2010, 53: 1247–1251
2 Cui B, Zhang X Q, Sun L, et al. A high-performance narrowband high temperature superconducting filter. Chin Sci Bull, 2010, 55: 1367–1371
3 Xia H H, Zhou C X, Zuo T, et al. Development of high-temperature superconducting filters operating at temperatures above 90 K. Chin Sci Bull, 2009, 54: 3596–3599
4 Gao L, Guo J, Wang Y H, et al. A 23 GHz high-temperature superconducting microstrip filter for radio astronomy. Chin Sci Bull, 2009, 54: 3485–3488
5 Wei B, Guo X B, Piao Y L, et al. Field test of HTS receivers on CDMA demonstration cluster in China. Chin Sci Bull, 2009, 54: 612–615
6 You L X, Shen X F, Yang X Y, et al. Single photon response of superconducting nanowire single photon detector. Chin Sci Bull, 2010, 55: 441–445
7 Wang J P, Li Y B, Kang L, et al. Design and fabrication of superconducting HEB mixer. Chin Sci Bull, 2009, 54: 2013–2017
8 Van D W C H, Ter H A C R, Wilhelm F K. Quantum superposition of macroscopic persistent-current states. Science, 2000, 290: 773–777
9 Mooij J E, Orlando T P, Levitov L, et al. Josephson persistent-current qubit. Science, 1999, 285: 1036–1039
10 Wirth T, Lisenfeld J, Lukashenko A, et al. Microwave readout scheme for a Josephson phase qubit. Appl Phys Lett, 2010, 97: 262508
11 Romans E J, Osley E J, Young L, et al. Three-dimensional nanoscale superconducting quantum interference device pickup loops. Appl Phys Lett, 2010, 97: 222506
12 Clarke J. Flux qubit completes the hat trick. Science, 2003, 299: 1850–1851
13 Clarke J, Wilhelm F K. Superconducting quantum bits. Nature, 2008, 453: 1031–1042
14 Chiorescu I, Nakamura Y, Harmans C J M P, et al. Coherent quantum dynamics of a superconducting flux qubit. Science, 2003, 299: 1869–1871
15 Orlando T P, Mooij J E, Tian L, et al. Superconducting persistent-current qubit. Phys Rev B, 1999, 60: 15398
16 Nakamura Y, Pashkin Y A, Tsai J S. Coherent control of macroscopic quantum states in a single-Cooper-pair box. Nature, 1999, 398: 786–788
17 Blatter G, Geshkenbein V B, Ioffe L B. Design aspects of superconducting-phase quantum bits. Phys Rev B, 2001, 63: 174511
18 Chiorescu I, Bertet P, Semba K, et al. Coherent dynamics of a flux qubit coupled to a harmonic oscillator. Nature, 2004, 431:159–162
19 Friedmann J R, Patel V, Chen W, et al. Quantum superposition of distinct macroscopic states. Nature, 2000, 406: 43–46
20 Lotkhov S V, Tolkacheva E M, Balashov D V, et al. Low hysteretic behavior of $Al/AlO_x/Al$ Josephson junctions. Appl Phys Lett, 2006, 89: 132115
21 Lang K M, Nam S, Aumentado J, et al. Banishing quasiparticles from Josephson-junction qubits: Why and how to do it. IEEE Trans Appl Supercond, 2003, 13: 989–991
22 Berkley A J, Xu H, Gubrud M A, et al. Decoherence in a Josephson-junction qubit. Phys Rev B, 2003, 68: 060502
23 Dolan G J. Offset masks for lift-off photoprocessing. Appl Phys Lett, 1977, 31: 337–339
24 Holmqvist T, Meschke M, Pekola J P. Double oxidation scheme for tunnel junction fabrication. J Vac Sci Technol B, 2008, 26: 1021–1023

Open Access This article is distributed under the terms of the Creative Commons Attribution License which permits any use, distribution, and reproduction in any medium, provided the original author(s) and source are credited.